Flow cytometric determination of size and complex refractive index for marine particles: comparison with independent and bulk estimates

Rebecca E. Green, Heidi M. Sosik, Robert J. Olson, and Michele D. DuRand

We advance a method to determine the diameter D and the complex refractive index ($n + n'i$) of marine particles from flow cytometric measurements of forward scattering, side scattering, and chlorophyll fluorescence combined with Mie theory. To understand better the application of Mie theory with its assumptions to flow cytometry (FCM) measurements of phytoplankton cells, we evaluate our flow cytometric-Mie (FCM-Mie) method by comparing results from a variety of phytoplankton cultures with independent estimates of cell D and with estimates of n and n' from the inversion of bulk measurements. Cell D initially estimated from the FCM-Mie method is lower than independent estimates, and n and n' are generally higher than bulk estimates. These differences reflect lower forward scattering and higher side scattering for single-cell measurements than predicted by Mie theory. The application of empirical scattering corrections improves FCM-Mie estimates of cell size, n, and n'; notably size is determined accurately for cells grown in both high- and low-light conditions, and n' is correlated with intracellular chlorophyll concentration. A comparison of results for phytoplankton and mineral particles suggests that differences in n between these particle types can be determined from FCM measurements. In application to natural mixtures of particles, eukaryotic pico/nanophytoplankton and *Synechococcus* have minimum mean values of n' in surface waters, and nonphytoplankton particles have higher values of n than phytoplankton at all depths.

OCIS codes: 010.4450, 120.4640, 260.2510, 290.4020, 290.5850, 350.4990.

1. Introduction

The properties of the suspended particulate matter in the upper ocean are an important determinant of optical variability,[1–3] affecting how sunlight is attenuated with depth in the ocean and how it is reflected from surface waters, two important factors in ocean-color algorithms. The primary factors that determine how a particle suspension interacts with the ambient light field include particle concentration and the distributions of size and complex refractive index ($n + n'i$). The complex refractive index is composed of a real part n that describes scattering at interfaces and an imaginary part n' that is indicative of the particle's light-absorption properties. Changes in particle properties affect the particle's inherent optical properties of absorption, scattering, and backscattering. For example, smaller particles and particles with higher values of n tend to have higher backscattering-to-scattering ratios. From simulations of the optical properties of oligotrophic waters, Stramski *et al.*[4] found that phytoplankton dominated absorption at most wavelengths mainly because of their high values of n', whereas inorganic particles were the most important contributors to both scattering and backscattering mainly because of their high values of n. From their simulation results, these authors concluded that an increased effort is needed to characterize the types and concentrations of particles suspended in seawater, both *in situ* and in the laboratory.

Flow cytometry is one of the few tools available for analyzing the optical properties of large numbers of individual particles. Flow cytometry (FCM) forward and side scattering, fluorescence, and labeling techniques can be used to enumerate, classify, and size various phytoplankton and nonphytoplankton particles.[5] With flow cytometry it is possible to enumer-

The authors are with the Woods Hole Oceanographic Institution, Department of Biology, Woods Hole, Massachusetts 02543. M. D. DuRand is also with Ocean Sciences Centre, Memorial University of Newfoundland, St. John's, Newfoundland A1C 5S7, Canada. H. M. Sosik's email address is hsosik@whoi.edu.

Received 21 May 2002; revised manuscript received 23 October 2002.

0003-6935/03/030526-16$15.00/0

ate and distinguish specific groups of particles in the ocean including *Prochlorococcus*, *Synechococcus*, eukaryotic picophytoplankton and nanophytoplankton, coccolithophorids, pennate diatoms, cryptophytes, and heterotrophic bacteria.[5–7] Cell size has been estimated from empirical relationships between FCM forward scattering and cell volume developed for laboratory cultures[7–9] and field populations of phytoplankton.[10] As well, cell size has been determined from FCM scattering and with a time-of-transit measurement through the illuminating beam, an approach that avoids the effects of cell refractive index on scattering versus volume relationships.[11]

In this paper we develop a method for determining size, n, and n' of individual particles with flow cytometry and Mie theory. We have advanced an approach first developed by Ackleson and Spinrad[12] who applied Mie theory to angular scattering measurements from flow cytometry to determine size and n for phytoplankton cells of less than 10-μm diameter. Given the size, n, and n' of a homogenous spherical particle, Mie theory describes how incident light is absorbed and scattered, including the angular distribution and polarization of the scattered light.[13] The method for applying Mie theory to flow cytometry involves a comparison of theoretical and measured angular scattering for particles of known size and/or n and n', including polystyrene beads and oil suspensions; we have added silica beads because they are within the range of n expected for phytoplankton cells. In addition to size and n we have incorporated the determination of n' for phytoplankton cells, from an empirical relationship between FCM chlorophyll red fluorescence and absorption cross section.[14]

Mie theory is the theoretical basis in our approach for determining the size and complex refractive index from FCM angular scattering and fluorescence measurements. Inherent in the theory are the assumptions that particles are spherical and homogenous, assumptions from which natural particles, such as phytoplankton cells, are known to deviate. Mie theory (or approximations of the theory) have previously been applied to bulk optical measurements to infer n and n' of phytoplankton cultures, and these values of n and n' have been within the ranges expected for phytoplankton and were correlated with intracellular carbon and chlorophyll concentrations.[4,15,16] Recently, Volten *et al.*[17] compared the angular distributions of light scattered by phytoplankton suspensions measured in the laboratory with Mie theory estimates of angular scattering based on bulk optical determinations of n and n', and they found significant differences between measured and theoretical angular scattering. They suggested that these deviations were due to phytoplankton not being homogenous spheres, as assumed for Mie calculations. Perhaps for this reason Ackleson *et al.*[18] observed that their estimates of n from single-cell optical measurements tended to be higher than previously published estimates of phytoplankton n from bulk optical properties. Given these discrepancies we further investigated the accuracy of FCM determinations of size, n, and n' by comparing them to independent and bulk estimates of these values.

The purpose of our research is to improve on the application of Mie theory to FCM measurements to determine the properties of phytoplankton and nonphytoplankton particles in natural samples. The accurate determination of individual particle properties is necessary for interpreting the variability in bulk optical properties. We have developed a method for determining cell diameter, n, and n' from single-particle measurements on the basis of validation with independent and bulk estimates of these values for cultures of phytoplankton. Although phytoplankton cells are known to deviate from the assumptions of Mie theory, we wished to explore whether using the theory would improve our ability to characterize natural particles compared with previous purely empirical approaches. We found that the successful application of Mie theory to phytoplankton depends on the characterization of how their forward and side scattering compares with that of spherical, homogenous particles, an assumption inherent in the theory. Our modified approach for the analysis of individual particle measurements improved the determination of cell properties for different species of phytoplankton and in different growth conditions. For nonphytoplankton particles we used our method to determine diameter and n. However, assumptions need to be made for n' and how the scattering of these particles relates to that of homogenous spheres. We applied our method to natural mixtures of particles containing phytoplankton and nonphytoplankton from New England continental shelf waters to exemplify how particle properties vary in natural samples.

2. Methods for Particle Measurements

A. Flow Cytometry

A modified Epics V flow cytometer (Coulter Electronics Corporation) interfaced with a Cicero acquisition system (Cytomation, Inc.) was used to measure forward light scattering (FLS) (~3–19° at 488 nm), side light scattering (SSC) (~54–126° at 488 nm), chlorophyll fluorescence (CHL) (660–700 nm), and the concentration of particles. The dynamic range of FLS, SSC, and CHL measurements was increased by splitting the optical signals and independently detecting and amplifying them with separate photomultipliers and three-decade logarithmic amplifiers. For each property the relative sensitivities of the two measurements were adjusted to have a one-decade overlap, and thus the potential measurement range was expanded to 5 orders of magnitude. Particles were injected into a saline sheath flow and illuminated by light from an argon-ion laser beam polarized parallel to the fluid stream. The samples were delivered with a peristaltic pump (Harvard Apparatus), and cell concentration was determined from pump flow rate and sample analysis time. Polystyrene microspheres of various sizes (from 0.57 to 6.2 μm YG beads from Polysciences, Inc.) were measured as reference particles. Data were saved as listmodes and

analyzed with a version of CYTOWIN software (originally written by D. Vaulot, http://www.sb-roscoff.fr/Phyto/cyto.html) modified to merge data from two logarithmic amplifiers. For populations of beads and cultured cells the arithmetic means of FLS, SSC, and CHL were computed following the transformation of distributions to linear values. All values of FLS, SSC, and CHL were normalized to values for the 2.14-μm beads.

B. Absorption and Attenuation

The spectral absorption coefficients a of phytoplankton suspensions were measured on a Perkin-Elmer Lambda 18 UV/VIS spectrophotometer equipped with a 60-mm integrating sphere. Samples were placed in a 1-cm quartz cuvette at the entrance to the integrating sphere, and measurements were made over the spectral range of 300–900 nm with a speed of 240 nm s^{-1}, a slit width of 4 nm, and a scan interval of 1 nm. The optical density of cultures was measured relative to syringe-filtered (0.22 μm) culture or fresh media (depending on the experiment) in the reference cuvette. A dilution series was measured at the start of each experiment to ensure that in subsequent measurements the multiple-scattering effects were negligible. All spectra were offset to zero optical density at 750 nm.

A flow-through absorption and attenuation meter with a 25-cm path length (ac-9, WETLabs) was used to measure the spectral beam attenuation coefficient c at nine wavelengths (412, 440, 488, 510, 532, 555, 650, 676, and 715 nm). Two reservoirs were attached with tubing to the inlet and outlet of the ac-9, samples were gravity fed through the instrument, and data collection was monitored to ensure the absence of air bubbles. Filtered seawater was used to dilute phytoplankton cultures before measurement and was analyzed between samples and subtracted as a blank. A dilution series was measured at the start of the experiment to ensure that there were no concentration-dependent effects on the measurements. During data processing, temperature correction was applied to account for the difference between water temperature at the time of sampling and during instrument calibration.[19] The values of a measured with the spectrophotometer and ac-9 were similar, and we chose to use the spectrophotometric values since they are less susceptible to noise and other sampling errors.

C. Ancillary Measurements

Cell-size distributions were determined with a Coulter Multisizer (Coulter Corporation) equipped with either a 30-, 50-, or 100-μm aperture, depending on the size of the cells. The instrument was calibrated with 5.11-, 9.32-, and 19.61-μm microspheres for the 30-, 50-, and 100-μm apertures, respectively. Cultures were diluted with filtered seawater to obtain coincidence rates of 6% or less. The size distributions of replicate samples were averaged and normalized to the cell concentration from FCM analysis. Size distributions of the smaller cells were fit with a Gaussian curve to extrapolate distributions where the signal-to-noise ratio was low. The 256-channel data of cell-diameter distributions were used to calculate the diameter of the mean cell D and the geometric projected area of the mean cell to include the effects of polydispersion in our calculations.[20,21]

Duplicate samples of 1–2 ml of culture were filtered onto *GF/F* filters and frozen in liquid nitrogen for later fluorometric chlorophyll a analysis. The fluorometer (Turner 10-AU with optical filter kit 10-040R) was calibrated with a dilution series of pure chlorophyll a (Sigma Chemical Company) in 90% acetone. Filtered samples were removed from liquid nitrogen, extracted overnight in cold 90% acetone, agitated, and the supernatant was removed after 5 min in a clinical centrifuge ($\sim 4000 \times g$). Fluorometer readings were made before and after acidification to account for the effects of phaeophytin in the calculation of chlorophyll a concentration.[22] Consistent with previous work[23] we found that our extraction approach was ineffective for *Nannochloris* sp. and two unidentified eukaryotes (t6 and isb), all of which are small (<3-μm) cells containing chlorophyll b. These species were excluded from data analysis involving chlorophyll relationships.

Duplicate 25-ml samples of each culture were also filtered onto precombusted *GF/F* filters, frozen, and later dried overnight at 60 °C before analysis on a Perkin-Elmer 2400 CHN analyzer with acetanilide as the standard. Carbon values of wet and dry filter blanks were a few percent of sample carbon signals and were subtracted from sample values. Intracellular carbon concentration (kg m^{-3}) was calculated by averaging replicate samples and dividing raw carbon values by volume filtered, cell concentration, and mean cell volume.

D. Particle Types

We compiled a data set of physical and optical measurements for numerous types of phytoplankton ranging in size from 1 to 10 μm, polystyrene and silica microspheres (beads), suspensions of oil droplets, and clay minerals. FCM measurements were made of oils and beads as reference particles to calibrate the application of Mie theory to our FCM configuration. Phytoplankton data were derived from a combination of several laboratory experiments as well as from analysis of natural seawater samples, and a variety of measurements were made on them as described below. As well, FCM measurements were made of clay mineral suspensions to compare angular scattering by organic and inorganic particles.

We divided our phytoplankton laboratory experiments into correction and application data sets for which measurements were made independently (Tables 1 and 2). An empirical correction for determining cell D, n, and n' from Mie theory and flow cytometry was developed from the correction data set, and then the correction was evaluated by applying it to the application data set. The correction data set included ten species of phytoplankton, for which all particle measurements were made. The

Table 1. Specifications for Cultures in the Correction Data Set[a]

Phytoplankton Species	D (μm)	Bulk Estimates			
		Q_a	Q_c	n	n'
Synechococcus sp. (7d95m)	1.21	0.11	0.98	1.063	0.0033
Unidentified eukaryote (isb)	1.27	0.30	2.50	1.12	0.0098
Unidentified eukaryote (t6)	2.19	0.25	2.81	1.075	0.0052
Nannochloris sp.	2.59	0.23	2.55	1.063	0.0039
Unidentified eukaryote (islow1)	2.61	0.33	2.21	1.056	0.0061
Isochrysis galbana	4.42	0.38	2.71	1.070	0.0041
Emiliania huxleyi (no coccoliths; Clone BT6)[b]	4.57	0.47	3.65	—	—
Thalassiosira pseudonana	4.81	0.22	2.36	1.032	0.0022
Monochrysis lutheri	5.26	0.37	2.38	1.065	0.0033
Dunaliella tertiolecta	7.93	0.55	2.64	1.037	0.0042

[a]Cultures were grown at a growth irradiance of 90 μmol photons m^{-2} s^{-1}.
[b]Culture excluded from analysis because no independent solution was found for n or n'.

application data set, which contained 22 cultures, differed from the correction data set in that the experiments were diel studies involving many measurements for the same species or because only a subset of particle measurements were made. The application data set contained 13 species of phytoplankton each grown at low-light levels and high-light levels (for experimental details for a subset of these cultures, see Shalapyonok *et al.*[24]). The application data set also included two diel studies of *Micromonas pusilla*[25] and *Nannochloris* sp.,[16] for which measurements were made every 2 h over a 24-h period. We did not include in our measurements phytoplankton cells that are far from spherical (e.g., pennate diatoms or chains of cells) or contained gas vacuoles; the measured cells had morphologies ranging from spherical to cylindrical with aspect ratios as high as 2. Considering all cultures, an average of 56,000 cells per culture was analyzed on the flow cytometer, and the mean coefficients of variation for FLS, SSC, and CHL were 16%, 20%, and 26%, respectively.

For the laboratory experiments, monospecific but nonaxenic cultures were grown in $f/2$ medium[26] in defined conditions of light intensity and temperature; various measurements were made. All cultures were grown in either natural light conditions (high

Table 2. Specifications for Cultures in the Application Data Sets

Phytoplankton Species	Light Level (μmol photons m^{-2} s^{-1})	D (μm)
Synechococcus sp. (WH8109)	50–100	0.93
Synechococcus sp. (WH7803)	50–100[a]	1.01
Synechococcus sp. (WH8012)	50–100[a]	1.10
Synechococcus sp. (WH8103)	50–100	1.13
Synechococcus sp. (7d95m)	Natural,[b] 70[b]	1.16
Micromonas pusilla	120[a,c]	1.63
Unidentified eukaryote (t6)	Natural, 70[b]	2.41
Pycnococcus provasolii	50–100[a]	2.63
Nannochloris sp.	Natural,[b] 70,[b] Natural,[c] 50–100[a]	2.68
Unidentified eukaryote (islow1)	Natural[b]	2.76
Minutocellus polymorphous (13DT11)	Natural[b]	3.72
Emiliania huxleyi (with coccoliths; Clone 12-1)	Natural,[b] 50–100	3.98
Unidentified eukaryote (t11)	Natural[b]	4.10
Isochrysis galbana	50–100[a]	4.72
Monochrysis lutheri	Natural,[b] 50–100[a]	5.10
Isochrysis sp.	Natural,[b] 70[b]	5.13
Emiliania huxleyi	Natural[b]	5.58
Dunaliella tertiolecta	Natural,[b] 70,[b] 50–100	7.81
Amphidinium carterae	50–100	9.25
Hymenomonas carterae	50–100[a]	9.29
Platymonas sp.	Natural[b]	9.66
Olisthodiscus sp.	Natural[b]	9.82

Note: The growth irradiance natural denotes cultures acclimated for growth in natural light during the summertime (June–August) in Woods Hole, Mass. When multiple irradiances are specified they refer to separate experiments.
[a]Cultures (in addition to the correction data set) used to determine the relationship between spectrophotometrically determined σ_a (488 nm) and FCM CHL (680 nm).
[b]Data from Shalapyonok *et al.*[24]
[c]Cultures for which diel measurements were made; data from DuRand and Olsen[16] and DuRand *et al.*[25]

light, summertime in Woods Hole, Mass.) or Cool-White fluorescent lights (low light, 50–120 μmol photons $m^{-2} s^{-1}$); all light levels were constant, except in the case of the natural light studies and the diel studies of *Micromonas* and *Nannochloris* for which cultures were grown under a 12:12 light:dark cycle. In each case the temperature was held constant at a value between 20 and 24 °C. A variety of measurements were made on cultures in either the exponential or the stationary phase of growth. For all cultures in the correction data set and for the two diel experiments in the application data set, a full suite of measurements was made, including FCM FLS, SSC, CHL, spectral a and c, Coulter Counter size distributions, and carbon concentrations; chlorophyll concentrations were measured only for cultures in the correction data set and the *Micromonas* diel experiment. Spectral c was measured with an ac-9 (as described above) except in the case of the *Nannochloris* diel experiment for which c was measured at 665 nm on a SeaTech transmissometer (25-cm path length). (The conversion to 488 nm is discussed below.) For all other cultures in the application data set a more limited set of measurements was made that included FCM FLS, SSC, CHL, Coulter Counter size distributions, and in some cases spectrophotometric measurements.

Oil suspensions were measured on the flow cytometry and used as calibration particles with known refractive index. Suspensions of heptane, nonane, or dodecane (Sigma Chemical Company) were made by adding a small amount of oil to a syringe of filtered seawater and shaking vigorously to form a polydispersion of droplet sizes.[12] Refractive indices of the oils were measured on a refractometer (Fisher Scientific) in the laboratory as 1.0325, 1.0467, and 1.0590 for heptane, nonane, and dodecane, respectively. (All refractive indices are discussed relative to seawater for which $n = 1.339$ relative to a vacuum.) These values differ slightly from those in the *CRC Handbook of Chemistry and Physics* (1998–1999) that were published as 1.0364, 1.0496, and 1.0617, respectively. The values measured on the laboratory refractometer gave accurate readings for a set of standards and were used in our analyses. The oils, which are colorless, were assumed to be nonabsorbing as in previous work (Ackleson and Spinrad[12]).

Beads of known size and refractive index were measured on the flow cytometry and used as calibration particles. Polystyrene beads of several sizes (0.57, 2.14, 2.9, 3.79, 5.2, and 6.2 μm) and n of 1.19 were analyzed in conjunction with each laboratory and field experiment. A silica bead of 1.58 μm (Duke Scientific, Inc.) was also included in the correction data set and *Micromonas* diel experiment and is of particular interest because its refractive index of 1.09 is closer than that of polystyrene beads to values within the plausible range for phytoplankton cells, generally from 1.01 to 1.10. Polystyrene-bead absorption was measured spectrophotometrically for the 2.14-μm bead and was calculated for the other sizes of polystyrene beads by multiplying by the ratio of each bead's mean FCM CHL to that of the 2.14-μm bead. In contrast to the polystyrene beads the silica beads are not manufactured with dyes so they were assumed to be nonabsorbing. Considering all beads, the mean coefficients of variation for FLS, SSC, and CHL were 4%, 7%, and 7%, respectively. Polystyrene and silica-bead suspensions were found to contain numerous other particles as well, such as bead fragments, fused beads, and doublets (despite sonication). These particles at other sizes can be present at significant concentration. For FCM measurements this is not an issue because the population at the size of interest is chosen in data analysis and all other particles are disregarded. However, obtaining a monodisperse population of beads for bulk analysis would be difficult.

Clay minerals were measured on the flow cytometry and were used to compare angular scattering by organic and inorganic particles. Four species of clay minerals were measured (University of Missouri Clay Repository): kaolinite (KGa-1b), montmorillonite (SAz-1), illite (IMt-1), and hectorite (SHCa-1). Mineral suspensions were made by adding a small amount of the sample to a syringe of filtered seawater and shaking vigorously to form a polydispersion of particle sizes. Ranges of n for each mineral type were determined from the *CRC Handbook of Chemistry and Physics* (1998–1999) as follows: kaolinite (1.14–1.17), montmorillonite (1.11–1.22), illite (1.15–1.20), and hectorite (1.11–1.13).

Selected field samples analyzed during the Coastal Mixing and Optics Experiment[27] were chosen to exemplify the application of our analyses to field data. The sampling site was located on the New England Shelf in 70 m of water at a single location (70° 30′ N, 40° 30′ W). We analyzed FCM samples collected during a noon depth profile on 6 May during a spring 1997 cruise.[28] FCM measurements were made on water samples collected with Niskin bottles on a rosette equipped with a conductivity-temperature-depth sensor. Eukaryotic pico/nanophytoplankton populations were discriminated from nonphytoplankton particles on the basis of their FCM CHL signal, and *Synechococcus* cells were discriminated by their orange fluorescence. With our methodology for applying Mie theory to FCM measurements, we analyzed each particle in a sample and created size and refractive-index distributions for eukaryotic phytoplankton, *Synechococcus*, and nonphytoplankton.

3. Theoretical Development

A. Mie Theory and Estimation of Bulk n and n'

Bulk estimates of n and n' at 488 nm were derived through an inverse method that uses Mie-scattering theory and/or an approximation of the theory. The cross sections for attenuation σ_c, absorption σ_a, and scattering σ_b were computed as the relevant bulk coefficients normalized to cell concentration [e.g., $\sigma_c = c/(N/V)$, where N/V is the number of cells per volume]. With the optical cross sections and mean cell diameter as inputs the dimensionless efficiency

factors for absorption Q_a and attenuation Q_c were calculated from the anomalous diffraction approximation[29] through iteration (following the approach described by Bricaud and Morel[30]). The value of n' was determined from

$$Q_a(\rho') = 1 + 2\,\frac{\exp(-\rho')}{\rho'} + 2\,\frac{\exp(\rho') - 1}{\rho'^2}, \quad (1)$$

where $n' = (\rho'/4)\{[2\pi(D/2)]/(\lambda/1.339)\}$. Once n' was determined, n was calculated through iteration from

$$Q_c(\rho) = 2 - 4\,\exp(-\rho\,\tan\,\zeta)\left[\frac{\cos\,\zeta}{\rho}\sin(\rho - \zeta) + \left(\frac{\cos\,\zeta}{\rho}\right)^2\cos(\rho - 2\zeta)\right] + 4\left(\frac{\cos\,\zeta}{\rho}\right)^2\cos\,2\zeta, \quad (2)$$

where ρ is the phase lag and $\tan\,\zeta = 1/2(\rho'/\rho)$. For the *Nannochloris* data set, n'(488 nm) and n (665 nm, wavelength of transmissometer, see Section 2) were derived from the anomalous diffraction approximation; n (665 nm) was converted to 488 nm by application of an average ratio observed between n at 665 nm and n at 488 nm for *Nannochoris* in the correction data set. For the correction data set and *Micromonas* diel experiment, the n and n' values were derived through an iterative procedure and optimization routines provided with the MATLAB software package (Mathworks, Inc.), in which the differences between Mie-modeled and measurement-derived Q_a and Q_c were minimized. The initial values of n and n' for the Mie-modeling approach were computed from the anomalous diffraction approximation. For cells in the correction data set that were >4 μm in diameter, two solutions were found for n, and the value was chosen that best fit the relationship of n versus the intracellular carbon concentration for all cells in the data set.

B. Mie Theory and Flow Cytometry

Our objective was to use Mie theory to infer particle D, n, and n' from FCM measurements of FLS, SSC, and CHL (for an overview, see Fig. 1). For this we need to know the particle's σ_a, the magnitudes of FLS and SSC, and the scattering angles associated with FLS and SSC. For phytoplankton, σ_a can be estimated from an empirical relationship with FCM CHL (see Section 4). We measure the magnitudes of FLS and SSC, but we do not know the optical geometry of FCM scattering precisely enough for the application of Mie theory. To infer the angles of FLS and SSC, we developed an optimization approach that uses FCM measurements of calibration particles and Mie theory calculations of scattering for these particles. The optimization allows for variation both in the range of angles contributing to FLS and SSC and in the weighting of contributions from different angles.

We performed an unconstrained, nonlinear minimization for calibration particles of known refractive index and/or size with optimization routines provided with the MATLAB software package. Embedded in our optimization is the program for Mie scattering that was provided by E. Boss and based on the FORTRAN code of Bohren and Hoffman,[31] and our application of Mie scattering to flow cytometry is a modification of a code originally written in FORTRAN by Ackleson and Spinrad.[12] Particles used in our optimization included polydisperse oil suspensions of heptane, nonane, and dodecane, polystyrene beads, and a silica bead. There were four variables in the optimization, two that were used to weight contributions to forward scattering (fls_1 and f_1) and two that were used to weight contributions to side scattering (ssc_1 and f_2). In both the forward- and side-scattering directions, light is scattered from a particle through the flow cell wall and collection lens and into the detector. For our FCM configuration, horizontal beam obscuration bars block the collection lens for both the forward- and side-scattering detectors, and additionally the entire lower half of the lens for the forward detector is obscured. The geometry of FLS scattering is sufficiently constrained for determination of an empirical function and, at a given angle, is based on the percentage of light that is obscured for a cone of light scattered from a particle and projected onto the forward detector. This leads to a weighting function for the forward detector of

$$w_{fls}(\theta) = f_1\left[1 - \frac{2fls_1}{\pi d\,\tan\left(\frac{2\pi\theta}{360}\right)}\right], \quad (3)$$

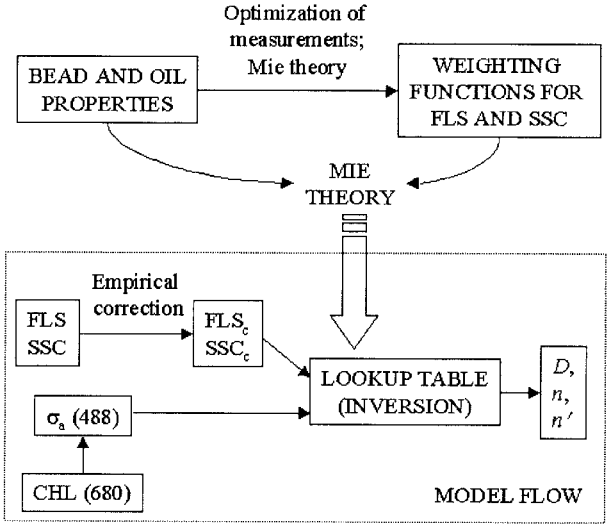

Fig. 1. Flow chart showing how D, n, and n' were derived from FCM measurements and Mie theory. The application of Mie theory to FCM measurements was optimized for measurements of standard particles (beads and oils) to develop weighting functions for FLS and SSC. The cell properties of D, n, and n' were determined from FLS$_c$, SSC$_c$, and σ_a from a lookup table, where FLS$_c$ and SSC$_c$ were calculated from FCM FLS and SSC by using empirical corrections derived for phytoplankton.

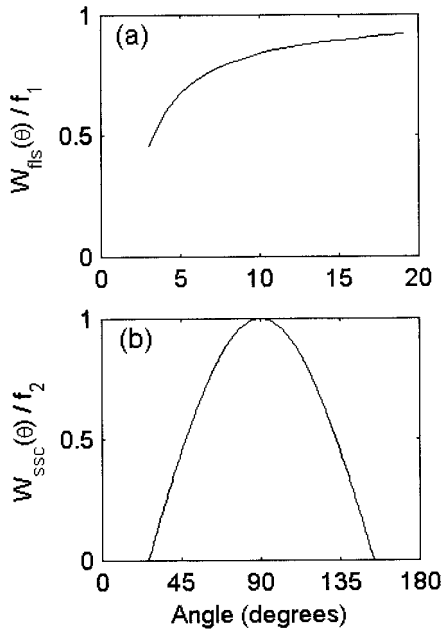

Fig. 2. Flow cytometric angular weighting functions for (a) forward scattering [$w_{fls}(\theta)$] and (b) side scattering [$w_{ssc}(\theta)$], normalized to the scalar multipliers f_1 and f_2, respectively [see Eqs. (3) and (4)]. The values of fls_1 = 1.11 mm and ssc_1 = 26° were used in Eqs. (3) and (4) according to results from our optimization approach applied to an average data set of oils and beads (see Section 4)]. The angular range for FLS was set to $3° \le \theta \le 19°$, whereas the angular range for SSC was determined by the optimized variable ssc_1.

where $3° \le \theta \le 19°$, d is the distance from the particle to the collection lens (= 24.9 mm), $fls_1 \approx 1/2$ the width of the obscuration bar, and f_1 is a scalar multiplier [Fig. 2(a)]. In contrast to FLS the collection of light scattered to the side angles is too complex to be defined empirically for our FCM configuration, and a sine function was chosen to represent the weighting for SSC because it provides good agreement between FCM measurements and Mie theory. The weighting for the side detector is described by

$$w_{ssc}(\theta) = f_2 \sin[\pi(w_a\theta + w_b)/180], \qquad (4)$$

where $ssc_1 \le \theta \le (180\text{-}ssc_1)$, $w_a = 180/(180\text{-}2*ssc_1)$, $w_b = -w_a*ssc_1$, and f_2 is a scalar multiplier [Fig. 2(b)]. As in Ref. 27, differential scattering cross sections in the FLS and SSC directions were calculated by multiplying the FLS and SSC weightings, $w_{fls}(\theta)$ and $w_{ssc}(\theta)$, by the first two elements of the scattering matrix to account for a polarized source (S11 and S12 in the notation of Bohren and Hoffman[31]) and by summing over all angles contributing to detected scattering signals. The first two elements of the scattering matrix, S11 and S12, are functions of S1 and S2 that are obtained directly from Mie theory. All values of FLS and SSC were normalized to angular scattering by a reference bead (a 2.14-μm polystyrene bead); in the case of Mie-modeled angular scattering the same weighting functions were used for the reference bead as determined above.

C. Development and Testing of the Flow Cytometer-Mie Method

With the weighting function results from this optimization a three-dimensional lookup table of Mie-theory-based solutions for particle FLS, SSC, and σ_a was created over the expected ranges of particle D (0–10 μm at a 0.1-μm resolution), n (1–1.10 at a 0.002 resolution; 1.10–1.30 at a 0.005 resolution), and n' (0–0.010 at a 5×10^{-4} resolution; 0.010–0.030 at a 1×10^{-3} resolution) for the marine particles of interest (i.e., phytoplankton cells, detritus, and minerals) (Fig. 1). For each particle, measured values of FLS, SSC, and σ_a can be compared with values in the lookup table and a solution (i.e., associated with values of D, n, and n') chosen by finding the minimum distance where

$$\begin{aligned}\text{distance} = &[\log_{10}(\text{FLS}_t) - \log_{10}(\text{FLS}_o)]^2 \\ &+ [\log_{10}(\text{SSC}_t) - \log_{10}(\text{SSC}_o)]^2 \\ &+ [\log_{10}(\sigma_{a,t}) - \log_{10}(\sigma_{a,o})]^2, \qquad (5)\end{aligned}$$

where the subscripts o and t refer to observed and theoretical values (i.e., from the lookup table), respectively. Forward and side scattering are normalized to that of a reference bead. The absorption cross section is represented by $\sigma_{a,o}$ and $\sigma_{a,t}$. At the position of minimum distance between the observed and theoretical values, D, n, and n' are chosen from the lookup table as the particle's estimated properties. We refer to this approach for applying Mie theory to FCM measurements as the flow cytometry-Mie (FCM-Mie) method.

4. Results and Discussion

A. Single-Particle Absorption

Phytoplankton absorption for laboratory and natural samples was calculated from FCM CHL. A regression was determined between spectrophotometrically derived σ_a (m^2 $cell^{-1}$) at 488 nm and FCM CHL at 680 nm; this regression was based on results for 14 phytoplankton species (25 cultures) measured in the laboratory, including all of the correction data set and a subset of the application data set (Table 2). The cultures used represent major taxonomic groups and range in size from 1 to 10 μm. A high correlation was observed between σ_a and FCM CHL (r^2 = 0.96 with a power function; Fig. 3). When the regression was applied to FCM CHL values for the cultures, a mean error of 30% was observed between modeled and measured σ_a. Previously, a relationship between FCM CHL and σ_a was described by Perry and Porter[14] who reported a strong correlation between FCM CHL and σ_a for 16 phytoplankton species (46 cultures; r^2 = 0.93).

B. Flow Cytometry and Mie Theory Optimization

We applied our optimization routine for deriving weighting functions that match FCM and Mie theory scattering (see Section 2) to measurements of oils and beads made during each phytoplankton experiment.

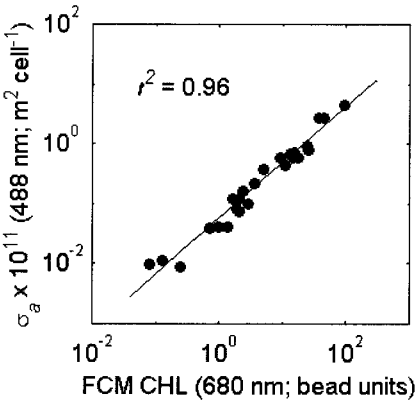

Fig. 3. Relationship between spectrophotometrically determined absorption cross section σ_a (488 nm) and flow cytometrically determined chlorophyll fluorescence, FCM CHL (680 nm), for a variety of phytoplankton species (Tables 1 and 2). Four of the 25 cultures used to determine this relationship are cyanobacteria.

Little difference was seen between oils and beads measured for each experiment in the correction and application data sets even though there were often months to years between measurements. Thus one optimization was performed on an averaged data set of oil and bead FLS and SSC measurements. We found good agreement between theoretical and measured FLS and SSC, especially in the size range of phytoplankton cells of interest, between 1 and 10 μm (Fig. 4). Significant deviation of the oil measurements from theory does not occur until below approximately 1 μm and above 15 μm. For the silica and polystyrene beads the mean deviation between theory and measurements was 7% for logarithmic values of FLS and 5% for logarithmic values of SSC [reported on a logarithmic scale because these are the values considered in Eq. (5)].

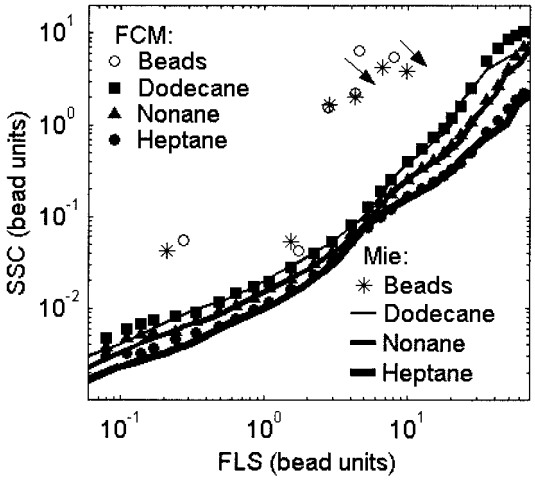

Fig. 4. Comparison of theory-based estimates and measurements of forward light scattering, FLS, and side light scattering, SSC, for beads and oil dispersions. The bead and oil measurements are an averaged data set over all experiments in the correction and application data sets. Several bead types were used in this comparison including 0.66-, 2.9-, 3.79-, 5.2-, and 6.2-μm polystyrene beads and 1.58-μm silica beads. Oil dispersions of heptane, nonane, and dodecane are shown. In cases in which the correspondence between FCM and Mie bead points is not obvious (i.e., the 5.2- and 6.2-μm polystyrene beads), the arrows show the match between bead points.

From the weighting function optimization and the resulting Mie-based lookup table, estimates of bead D, n, and n' from the FCM-Mie method were compared with known values. A comparison between the FCM-Mie estimates of D, n, and n' and measured values for all polystyrene beads analyzed resulted in the FCM-Mie method underestimating D by an average of 6%, overestimating n by 29%, and overestimating n' by 48%. For the silica bead the FCM-Mie method overestimated D by 14%, underestimated n by 20%, and accurately determined n'. The errors in n and n' for the polystyrene beads were larger than expected possibly because the relationship between FLS and SSC predicted from Mie theory is complicated at the higher value of n associated with the polystyrene beads (n = 1.19). Because phytoplankton cells are in the range of n for organic particles (n = 1.02–1.10), the lower errors associated with the silica bead and better fit for oil suspensions (Fig. 4) should be more representative of the application of the FCM-Mie method to phytoplankton. Note, however, that the actual errors for phytoplankton cells may be larger because they are not spherical and homogenous particles.

C. Evaluation of Method (for Phytoplankton)

To evaluate the validity of the FCM-Mie solutions, we compared estimates of D, n, and n' with other estimates of these values from measurements of phytoplankton cultures in the laboratory. Only cells of less than 10 μm in size were used owing to the limitations of our FCM approach that uses Mie theory and because it is difficult to determine independent values of n from bulk optical measurements for larger cells because unique solutions cannot be found.

Initially the values of D, n, and n' estimated from the FCM-Mie method were compared with independent estimates of D and bulk determinations of n and n' for the correction data set (Table 1). The culture of *Emiliania huxleyi* was excluded from analysis because no bulk solution was found for n or n'. For the 10 species of phytoplankton studied, the cell D values were underestimated [slope = 0.9 forced through zero; Fig. 5(a)], and n and n' values were generally overestimated [slope = 1.5 and 1.7, forced through one and zero, respectively; Figs. 5(b) and 5(c)]. The unidentified culture denoted isb was not included in the statistics for n and n', because its bulk estimate of n of 1.12 is considered to be outside the range plausible for phytoplankton cells. One explanation for the high value of n for this culture could be the presence in the sample of nonphytoplankton particles, such as bacteria or cell debris, for which concentrations were not measured.

We have confidence in our bulk values of n and n', because bulk estimates of n at 488 nm were well correlated with intracellular carbon concentration

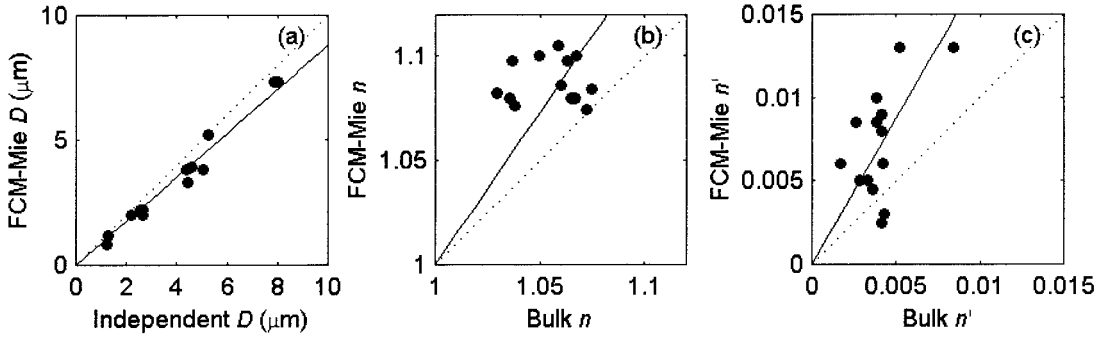

Fig. 5. Results for cultures in the correction data set (see Table 1). Comparison is shown between cell properties, (a) mean diameter D, (b) real refractive index n, and (c) imaginary refractive index n', estimated with the FCM-Mie approach and with independent and bulk methods. Independent D is from electronic particle counter measurements, and bulk n and n' are determined from the inversion of bulk optical measurements: dotted lines, 1:1 lines; solid lines, linear regression forced through zero in the case of D and n' and through one in the case of n.

($y = 2894.1x - 2819$, $r^2 = 0.61$, $n = 14$, data not shown), and bulk estimates of n' at 675 nm were correlated with intracellular chlorophyll concentration ($y = 653.99x + 0.617$, $r^2 = 0.47$, $n = 11$). These findings agree with previous work by Stramski,[32] who reported intracellular carbon concentration to be correlated with n at 660 nm and intracellular chlorophyll concentration to be correlated with n' at 675 nm for *Thalassiosira pseudonana* and *Synechococcus*. One explanation for the differences that we observe between FCM-Mie and independent and bulk determinations of D, n, and n' is that the FCM-Mie method depends on the quantification of angular scattering (FLS and SSC), which may be more highly affected by the deviation of phytoplankton cells from the Mie assumptions of sphericity and homogeneity compared with the independent and bulk property estimates. Another possibility is that cell D was underestimated by the FCM-Mie method, because elongated particles are oriented in flow in the flow cytometer so that a smaller diameter would be inferred from FCM scattering. When cell D is underestimated a higher value of n needs to be invoked to account for measured values of FLS and SSC, which could explain overestimated values of n determined from the FCM-Mie method.

In an effort to characterize and correct for the deviations between FCM-Mie and independent and bulk estimates of cell properties we investigated the relationship between modeled and flow cytometrically measured FLS and SSC. The modeled values of FLS and SSC were calculated from Mie theory with measurements of D and bulk estimates of n and n'. The FCM measurements of FLS were generally lower than modeled FLS by an average of 39%. The opposite trend existed for SSC with measurements generally higher than modeled values by an average of 19%. A second-order polynomial fit between logarithmic values of modeled and measured FLS gave a high correlation coefficient [$r^2 = 0.96$; Fig. 6(a)]. For SSC there was not a simple relationship between measured and modeled values, so we used a linear fit (forced through the position of *Synechococcus*) to describe the general bias; this fit explained 40% of the total variance [Fig. 6(b)]. Our general findings for SSC agree with those of Volten *et al.*[17] who found that, for 13 of the 15 phytoplankton cultures that they analyzed, measured polarized scattering at the side angles was significantly higher

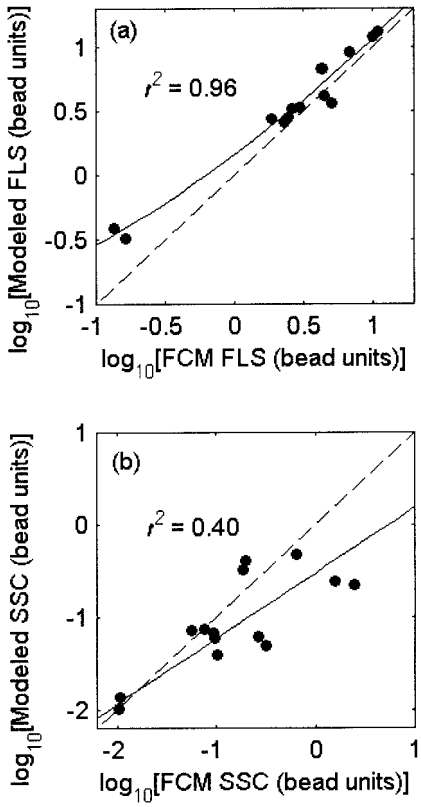

Fig. 6. Relationships between flow cytometrically measured and Mie-modeled values of (a) forward light scattering, FLS, and (b) side light scattering, SSC, for the correction data set (Table 1). Mie-modeled FLS and SSC values were determined from independent estimates of D and bulk estimates of n and n': dashed lines, 1:1 lines; solid lines, least-squares regression results between logarithmic-measured and modeled values.

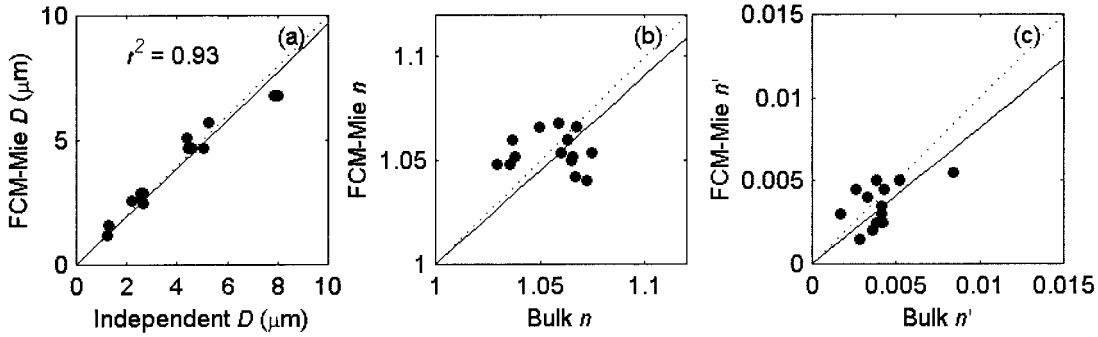

Fig. 7. Results for the correction data set (see Table 1). Comparison is shown between cell properties, (a) diameter D, (b) real refractive index n, and (c) imaginary refractive index n', estimated with the modified FCM-Mie method (i.e., with FLS_c and SSC_c) and with independent and bulk methods. The correlation coefficients for the n and n' relationships are not significant: dotted lines, 1:1 lines; solid lines, linear regression results.

than that estimated from Mie theory. Notably, and contrary to the general trend that we observed in SSC, the smallest cell that we measured, *Synechococcus*, had modeled values similar to or higher than the measured SSC values. Volten *et al.*[17] also found this trend for the two smallest cells that they measured, *Prochlorothrix hallandica* and *Selenastrum capricornutum*. Thus either there is some size dependence in the relationship between modeled and measured volume-scattering functions or smaller cells are more like homogenous spheres.

We used the regression results between modeled and measured FLS and SSC to calculate the corrected values of FCM FLS and SSC (FLS_c and SSC_c) before the particle measurements were compared with values in the Mie-based lookup table (Fig. 1). This represents a crude approach to account for general effects of the phytoplankton shape and structure. It cannot be expected to provide highly accurate results for every phytoplankton cell type but should provide improved estimates of D, n, and n' for many types. As expected, when applied to the correction data set, the results showed better agreement for all three parameters, D, n, and n' (Fig. 7). Cell D was the most accurately predicted of the three properties (slope = 1.0, r^2 = 0.93). The correlations between FCM-Mie and the bulk estimates of n and n' were still not significant, but the bias in the data was reduced (slope = 0.9 and 0.8 for n and n', respectively), and the mean values were more accurately predicted. Our relationship between the modeled and measured values for SSC has a higher variance than for FLS, most likely because FLS is highly dependent on diameter, whereas SSC is a more complex function of diameter, cell structure, and cell shape. This is supported by the fact that D is accurately predicted from FCM measurements for the correction data set with only an FLS correction, but that, to determine n and n', an SSC correction is also needed. Since the correction approach was developed with the correction data set, these results do not represent independent verification that the approach is reasonable; for this we used results from other experiments.

D. Laboratory Application

We evaluated our modified FCM-Mie approach (i.e., with corrected FLS and SSC, FLS_c and SSC_c) by applying it to independent data from the *Micromonas* and *Nannochloris* diel experiments.[16,25] For both species, cell D, n, and n' were better resolved by our FCM-Mie method with FLS and SSC corrections (Figs. 8 and 9). The mean errors in estimates of D were 4% and 6% for the *Micromonas* and *Nannochloris* diel experiments, respectively. Significant diel

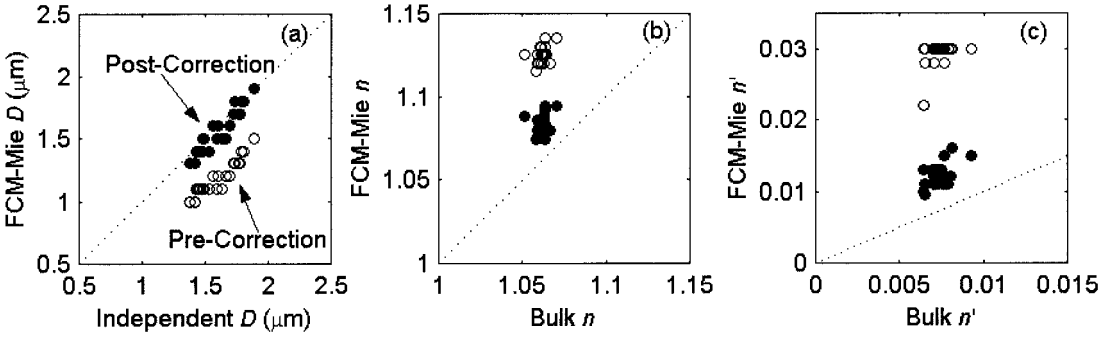

Fig. 8. Results for *Micromonas* sampled every 2 h over a 24-h period. Comparison is shown between cell properties, (a) diameter D, (b) real refractive index n, and (c) imaginary refractive index n', estimated with the modified FCM-Mie method and with independent and bulk methods. FCM-Mie estimates of D, n, and n' are shown, ○, before and, ●, after FLS and SSC corrections are applied: dotted lines, 1:1 lines.

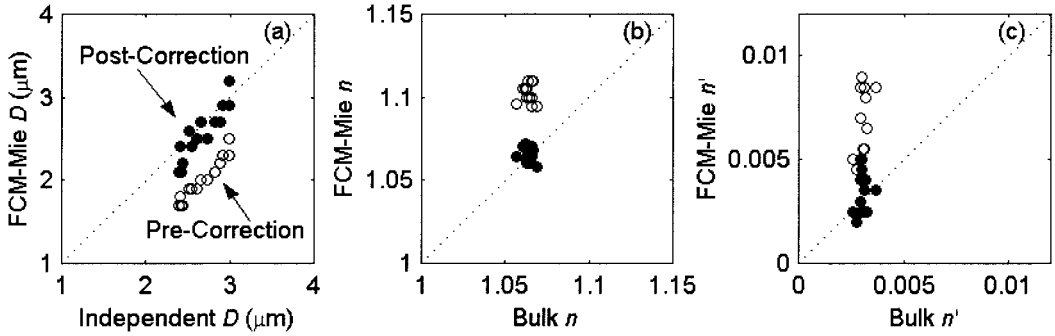

Fig. 9. Results for *Nannochloris* sampled every 2 h over a 24-h period. Comparison is shown between cell properties, (a) diameter D, (b) real refractive index n, and (c) imaginary refractive index n', estimated with the modified FCM-Mie method and with independent and bulk methods. FCM-Mie estimates of D, n, and n' are shown, ○, before and, ●, after FLS and SSC corrections are applied: dotted lines, 1:1 lines.

changes in D for both experiments were resolved by the FCM-Mie method ($r^2 = 0.90$ and 0.81 for linear fits). Previously we reported for these experiments that no consistent diel trends were observed in n and n' determined with bulk methods[16,25]; this is consistent with our observation that diel trends were generally not observed in FCM-Mie n and n'. The exception to this is that FCM-Mie values of n' for *Nannochloris* showed some indication of a diel pattern. Because no measurements of intracellular chlorophyll concentration were made for this experiment, we cannot assess whether the bulk or FCM-Mie values are more accurate in this case. Mean deviations between FCM-Mie and bulk n for the *Micromonas* and *Nannochloris* diel experiments were 35% and 8%, respectively, and mean deviations for n' were 67% and 22%, respectively. FCM-Mie n and n' were more accurately determined for *Nannochloris* than for *Micromonas*, because *Micromonas* is further from the regression line determined for the SSC correction. Further work on the scattering properties of *Micromonas* will be necessary to explain this observation.

Previously, the majority of FCM studies (with the exception of Ackleson *et al.*,[18] Ackleson and Spinrad,[12] and Ackleson and Robins[33]) have used FCM FLS to determine cell D from an empirical relationship with phytoplankton cell volume measured on an electronic particle counter.[7–9,24,34] For this approach, different empirical relationships are necessary to determine D for cells grown at low- and high-light levels (Fig. 10).[24] The high-light empirical relationship presented here was based on cells grown in high light from the application data set, and the low-light empirical relationship was based on cells grown in low light from the application data set. The high- and low-light empirical relationships predict significantly different estimates of cell D from FCM FLS and increasingly so as cell D increases. For example, for cells at the upper end of our diameter range of interest an FCM FLS of 15 gives a predicted cell D of 9.9 μm from the low-light empirical relationship and 7.4 μm from the high-light empirical relationship. At the smaller end of our diameter range of interest an FCM FLS of 1 corresponds to cell D of 2.1 μm from the low-light empirical relationship and 1.9 μm from the high-light empirical relationship.

We applied our FCM-Mie approach to data from the application data set to evaluate its performance with cultures grown under different light intensities and thus with different optical properties. Applying the FCM-Mie approach, we found that the resulting values of D were well correlated with measured values for cells grown under both high- and low-light intensities (Fig. 11; slopes = 0.97, $r^2 = 0.86$ and 0.98, respectively). In contrast the low-light empirical relationship (as discussed above) overestimates D for cultures grown in high light [Fig. 11(a); slope = 1.16], and a high-light empirical relationship underestimates D for cultures grown in low light [Fig. 11(b); slope = 0.73]. This result shows that the modified FCM-Mie method accounts for absorption and scattering so that we are able to predict accurately changes in cell size under different light regimes. The application of the FCM-Mie approach to the determination of D for cells grown at different light

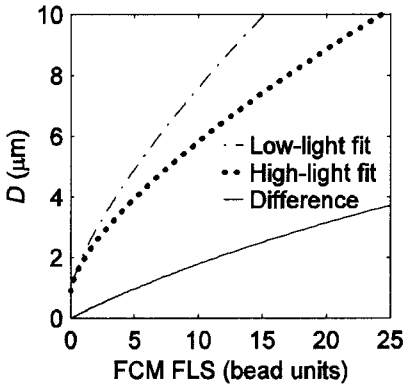

Fig. 10. Empirical relationships between FCM forward light scattering, FLS, and measured cell diameter D for cells grown in conditions of low- and high-light levels: solid curve, difference in D between the two fits as a function of FCM FLS. Similar empirical relationships were previously used for determining cell D from measurements of FCM FLS.

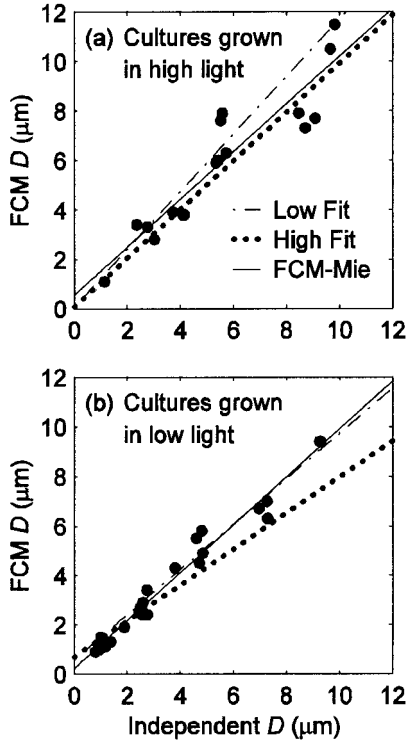

Fig. 11. Results for the application data set. Comparison is shown of cell diameter D estimates from the modified FCM-Mie method and from empirical relationships between FLS and measured cell D for cultures grown at (a) high and (b) low light. In each plot, lines for high-light calibration, low-light calibration, and FCM-Mie are linear regression results for cultures grown at high- and low-light levels, respectively; for clarity only the data points associated with the FCM-Mie approach are shown. The values of FCM-Mie D show a good correlation with independent D under both high- and low-light levels (slope, 0.97 in both cases), whereas the high- and low-light calibrations work well only for the intensities at which they were determined.

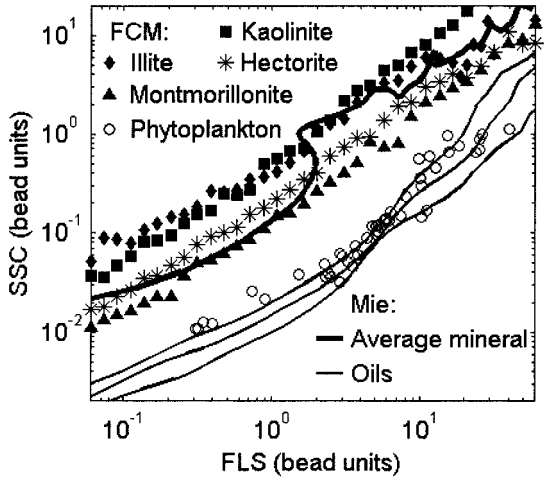

Fig. 12. Results of comparison of theory-based estimates and FCM measurements of forward light scattering, FLS, and side light scattering, SSC, for inorganic particles (minerals) and organic particles (phytoplankton cells and oil dispersions). Values of n for the different minerals are montmorillonite (1.11–1.22), hectorite (1.11–1.13), kaolinite (1.14–1.17), illite (1.15–1.20), and average mineral (1.18). The corrected values of FCM FLS and SSC (FLS_c, and SSC_c) are plotted for phytoplankton cultures from both the correction and the application data sets. The lines labeled Oils are theory-based estimates for heptane, nonane, and dodecane; the FCM-measured values are similar (see Fig. 4).

levels becomes increasingly important as cell size increases, as can be seen by the increasing deviation between the low- and high-light empirical fits with increasing cell D (Figs. 10 and 11).

We determined a level of confidence for each of the particle properties, D, n, and n', determined from the FCM-Mie method. All statistics involving the *Micromonas* and *Nannochloris* diel experiments include two points from each experiment at the values of the smallest and largest D. For the application data set (44 measurements of cultures grown at both low- and high-light levels) there was a mean error of 13% for D compared with measured values. The exact error in FCM-Mie n and n' could not be determined from comparison with bulk estimates of n and n', since both methods are based on inversion techniques that use Mie theory. We did compare the values of FCM-Mie n and n' with intracellular carbon and chlorophyll concentrations, however. For this comparison we used data from the correction data set and the *Micromonas* diel, because these were the only experiments for which carbon and chlorophyll concentrations were measured. We have confidence in values of n' determined from the FCM-Mie method because they are significantly correlated with intracellular chlorophyll concentration ($p = 0.002$), with a linear model explaining 60% of the variability. In comparison we have less confidence in the FCM-Mie values of n because they are not significantly correlated with intracellular carbon concentration even though the bulk estimates of n are. The higher apparent error in n compared with D is probably caused by higher unexplained variance in the SSC correction than in the FLS correction.

The comparison with bulk n and the intracellular carbon content suggests that we were able to determine the mean values of n by the FCM-Mie method that are reasonable, but we were not able to resolve the intraphytoplankton variability in n. Our FCM-Mie method should be useful for discriminating particles of low refractive index such as phytoplankton and organic detritus from particles of high refractive index such as minerals. We could not apply the FCM-Mie method to our mineral measurements in the same manner that we did for phytoplankton, because precisely defined size and refractive-index distributions were not available. However, we did measure polydisperse populations of several types of minerals and found that the values of FLS and SSC for these particles were within the range of values determined from Mie theory (Fig. 12). As well, the relationship between FLS and SSC for minerals was very different from that for organic particles, indicating that the FCM-Mie method should work well in resolving differences in n between organic and inorganic particles.

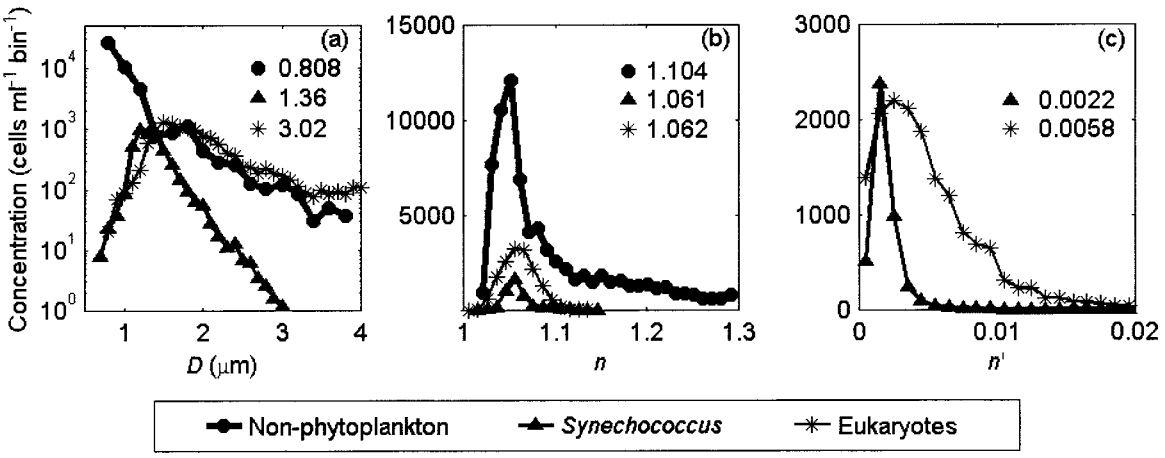

Fig. 13. Results for a sample from 1-m depth collected 6 May 1997 from New England shelf waters. The distributions of (a) diameter D, (b) real refractive index n, and (c) imaginary refractive index n' for *Synechococcus*, eukaryotic phytoplankton, and nonphytoplankton are estimated with the modified FCM Mie method. Mean values are indicated for each distribution. The n' distribution for nonphytoplankton is not plotted, because these particles are assumed to be nonabsorbing.

E. Field Application

We applied our methodology to natural samples collected 6 May 1997 in New England continental shelf waters. Distributions of D, n, and n' were computed for *Synechococcus* and eukaryotic pico/nanophytoplankton from measurements of FCM FLS, SSC, and CHL with the modified FCM-Mie method. For nonphytoplankton particles, absorption was assumed to be zero, and distributions of D and n were computed from FCM FLS and SSC with the FCM-Mie method without the FLS and SSC corrections determined for phytoplankton. The analysis was limited to particles of less than approximately 10 μm in size for both phytoplankton and nonphytoplankton. In size distributions for the surface sample, the populations of *Synechococcus* and eukaryotes had peaked distributions with mean D of 1.36 and 3.02 μm, respectively [Fig. 13(a)]. The nonphytoplankton increased in concentration with decreasing size with a Junge slope of 4.1, which is within the range of values (2–5 with 3–4 typical) previously reported for marine particle-size distributions (see references in Ref. 13). Given that we were not able to resolve intraphytoplankton variability in n for cultures, the distributions for phytoplankton n presented here for natural samples probably indicate both errors in our method and real variability in the scattering properties of cells; it is clear that further work is needed for an accurate quantification of n for cells. For the purpose of discussion, however, we consider that changes in mean n, even if not quantitatively precise, might indicate changes in scattering and thus physiological changes in cells. Real refractive-index distributions for *Synechococcus* and eukaryotes were in the range expected for phytoplankton (1.01–1.10), and the means (1.061 and 1.062, respectively) were approximately the same for the two populations [Fig. 13(b)]. Nonphytoplankton had a mean n of 1.104, which was higher than the mean n for the phytoplankton. Imaginary refractive-index distributions for *Synechococcus* and eukaryotes were in the range expected for phytoplankton [generally from 0 to 0.02 (Ref. 4)]; the mean value for *Synechococcus* of 0.0022 was lower than that for eukaryotes of 0.0058, presumably because *Synechococcus* contain phycoerythrin, a pigment that does not absorb at 488 nm as well as the accessory pigments of eukaryotes [Fig. 13(c)].[35] Distributions of D, n, and n' had a broader range for eukaryotes than for *Synechococcus*, as expected, because the eukaryotes comprise a broad range of species.

We also examined the depth dependence of particle properties in relation to the physical structure of the water column. Properties were estimated for each individual particle in a water sample, and then mean values were determined for each group of similar particles (i.e., *Synechococcus*, eukaryotes, and nonphytoplankton). The water column was thermally stratified with a surface mixed layer of ~16 m in which bulk chlorophyll fluorescence was elevated. For cases in which particle properties exhibited variation with depth, the mean D was higher within the mixed layer than below and mean n and n' were lower (Fig. 14). The depth distributions of D and n were more variable for eukaryotes than for *Synechococcus*, while n' changed approximately twofold with depth for both. Considering the mean property values within versus below the mixed layer, eukaryotes were 29% larger in surface waters (a difference of 0.87 μm) with a 14% lower n (a difference of 0.01) and a 49% lower n' (a difference of 0.0052). *Synechococcus* were 5% larger in surface waters (a difference of 0.066 μm) with a 51% lower n' (a difference of 0.002); n did not change significantly with depth for *Synechococcus*. Mean D, n, and n' were higher for eukaryotes than for *Synechococcus* at all depths, except for n within the mixed layer, which was not significantly different between the two groups. The mean nonphytoplankton particle was smaller and more refractive than the mean phytoplankton cell at all

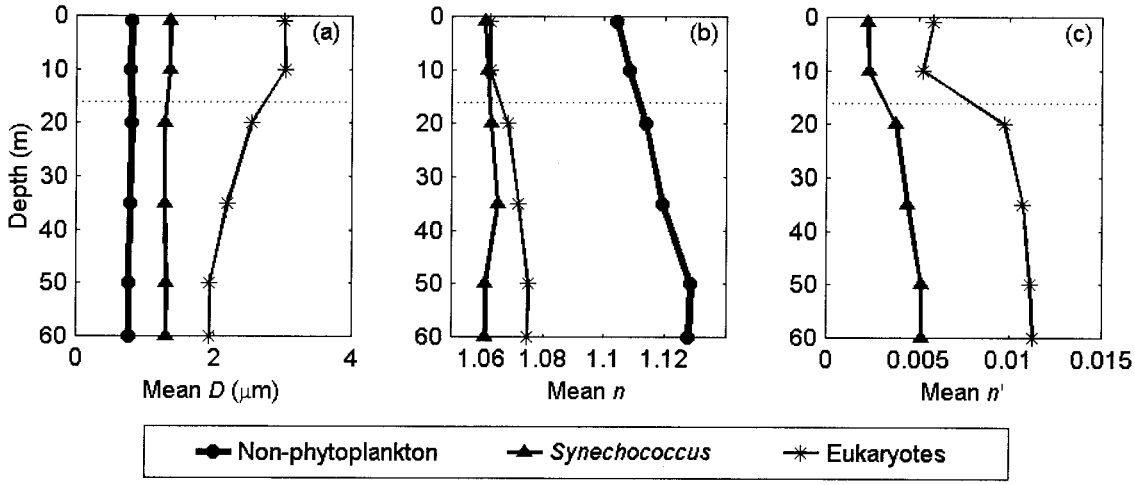

Fig. 14. Results for water samples collected 6 May 1997. Depth profiles of mean (a) diameter D, (b) real refractive index n, and (c) imaginary refractive index n', for *Synechococcus*, eukaryotic phytoplankton, and nonphytoplankton are estimated with the modified FCM-Mie method. The mean values were calculated from property distributions, which were in turn derived from an analysis of each particle in a sample: dashed lines, bottom of the mixed layer at 16-m depth.

depths. Nonphytoplankton mean D was 3% larger (a difference of 0.024 μm) within the mixed layer than below with a 13% lower mean n (a difference of 0.016).

Values of the real refractive index for nonphytoplankton should indicate the relative contributions of organic and inorganic particles. The mean n for nonphytoplankton (1.104–1.128) was higher than n for phytoplankton (1.0609–1.0751) at all depths. Compared with phytoplankton, these results imply that nonphytoplankton had a higher mineral content or, in the case of organic particles, a lower water content. Our findings are consistent with a recent study by Twardowski *et al.*[36] who employed an inverse method to derive the average real refractive index for natural particle assemblages from optical measurements and size distributions. In their study the values of n were generally lower in areas of high phytoplankton concentrations and higher in areas of high detrital content. In our example the values of n for nonphytoplankton were lower in the mixed layer than below, which is consistent with biological processes (e.g., cell death and the production of fecal material) as a source of organic particles within the mixed layer and resuspension of bottom sediments as a source of inorganic particles below the mixed layer. There are two caveats in the interpretation of nonphytoplankton n determined from the FCM-Mie method. First, we assumed that these particles were nonabsorbing, which is consistent with the low values of n' previously reported for organic detritus, of the order of 3×10^{-5} at 488 nm.[4] The values of n' for minerals, however, may be higher, on the order of 10^{-3}.[37] Second, and more important, we did not account for the effects of nonsphericity and inhomogeneities. The deviation of nonphytoplankton from homogenous spheres is a topic for further study and is complicated, because nonphytoplankton contain a broad range of different types of particles, including minerals, heterotrophic organisms, cell debris, and fecal matter.

The changes in average phytoplankton properties can be caused by changes at the cellular level and/or in the species composition of the population. The depth profile discussed here is associated with a stratified water column with decreased nutrient levels in the surface mixed layer and was collected near the end of a phytoplankton bloom in surface waters.[28] The differences seen in eukaryotic cell D, with the largest cells in surface waters, are most likely caused by differences in the species composition associated with the bloom within versus below the mixed layer. In contrast the variability in n' is more likely caused by changes at the cellular level that probably happen to all species owing to the effects of a stratified water column with high-light levels and low nutrients in surface waters compared with below the mixed layer. Values of n' for both eukaryotic phytoplankton and *Synechococcus* are lower in surface waters, which is consistent with previous findings that cells have less pigment per cell in conditions of high light and low nutrients (e.g., Refs. 38–40). The increase in n for eukaryotes with depth suggests that cells have higher intracellular carbon content below the mixed layer, which may be caused by changes in species composition and/or rearrangements in internal structures. In previous studies the modification of internal cell structures caused changes in angular scattering, especially at side angles[41,42]; these changes in scattering would presumably affect estimates of n and may be responsible for differences in eukaryotic n above and below the mixed layer.

5. Summary

We have developed a method for determining the D, n, and n' of marine particles from the FCM measurements of FLS, SSC, and CHL combined with Mie theory. Particles of known D, n, and n' were mea-

sured to characterize FCM parameters before they were used in Mie calculations. An empirical laboratory calibration, involving a variety of phytoplankton species, was used to convert from FCM CHL to σ_a at 488 nm. For each particle the FCM measurements of FLS, SSC, and CHL were compared with the values in a Mie-based lookup table to determine D, n, and n'. From the initial comparison of these D, n, and n' values with independent values from electronic particle counter data and inversion from bulk optical measurements, we found that cell D was underestimated and n and n' were overestimated by the FCM-Mie method. For phytoplankton cells the FLS and SSC empirical corrections were determined from a comparison of FCM measurements and modeled values; these corrections were necessary to determine accurately cell properties from the FCM-Mie method. The FLS and SSC corrections were probably necessary because cells deviate from the Mie theory assumptions of particle sphericity and homogeneity.

Our modified FCM-Mie method (i.e., with FLS and SSC corrections) improved the determination of phytoplankton cell properties for a variety of cultures. The FCM-Mie method provided estimates of cell D to within 13% of directly measured values, and the estimates were better than those obtained from the empirical correlation of FLS with cell D. Notably D could be determined accurately for cells grown in both high- and low-light conditions, despite different FLS:D relationships for these two conditions. FCM-Mie estimates of n and n' were not correlated with bulk estimates but were within the range expected for phytoplankton cells, and values of FCM-Mie n' were significantly correlated with intracellular chlorophyll concentration. With our method we were not able to resolve intraphytoplankton variability in n. However, the FCM-Mie method is useful for discriminating between organic and mineral particles. Improving the determination of the refractive index of individual particles by flow cytometry requires additional measurements, such as time-of-flight and pulse-shape analyses, to provide information about cell shape and internal heterogeneity.

In future work we will apply our FCM-Mie methodology to determining spatial and temporal changes in D, n, and n' for phytoplankton and nonalgal particles, including bacteria, organic detritus, and minerals, measured during both summer 1996 and spring 1997 in New England continental shelf waters. We expect that estimates of individual particle properties will help explain the variability in bulk inherent and apparent optical properties. The application of our FCM-Mie method to natural assemblages should improve our understanding of how intraparticle variability (changes in D, n, and n') and interparticle variability (changes in the relative concentrations of particle types) contribute to changes in bulk optical properties in the ocean.

This work was supported by Office of Naval Research (ONR) grants N00014-95-1-0333 and N00014-96-1-0965 (H. Sosik and R. Olson) and a NASA Earth System Science Fellowship (R. Green). We thank A. Canaday and A. Shalapyonok for assistance in the laboratory, A. Solow for help with statistical computations, S. Ackleson and E. Boss for Mie-scattering programs, and H. Volten for making angular scattering data available. We also thank C. Mobley and S. W. Chisholm for comments on an early draft of the manuscript and two anonymous reviewers who provided critical comments that improved this work. This is Woods Hole Oceanographic Institution contribution 10718.

References

1. A. Morel and L. Prieur, "Analysis of variations in ocean color," Limnol. Oceanogr. **22,** 709–722 (1977).
2. J. T. O. Kirk, *Light and Photosynthesis in Aquatic Ecosystems* (Cambridge University, New York, 1983).
3. M. R. Lewis and J. J. Cullen, "From cells to the ocean: satellite ocean color," in *Particle Analysis in Oceanography*, S. Demers, ed. (Springer-Verlag, New York, 1991), pp. 325–337.
4. D. Stramski, A. Bricaud, and A. Morel, "Modeling the inherent optical properties of the ocean based on the detailed composition of the planktonic community," Appl. Opt. **40,** 2929–2945 (2001).
5. R. J. Olson, E. R. Zettler, and M. D. DuRand, "Phytoplankton analysis using flow cytometry," in *Aquatic Microbial Ecology*, P. F. Kemp, B. F. Shen, E. B. Shen, and J. J. Cole, eds. (Lewis Publishers, Boca Raton, Fla., 1993), pp. 175–186.
6. D. Marie, F. Partensky, S. Jacquet, and D. Vaulot, "Enumeration and cell cycle analysis of natural populations of marine picoplankton by flow cytometry using the nucleic acid stain SYBR Green I," Appl. Environ. Microbiol. **63,** 186–193 (1997).
7. R. J. Olson, E. R. Zettler, and O. K. Anderson, "Discrimination of eukaryotic phytoplankton cell types from light scatter and autofluorescence properties measured by flow cytometry," Cytometry **10,** 636–643 (1989).
8. M. D. DuRand, "Phytoplankton growth and diel variations in beam attenuation through individual cell analysis," Ph.D. dissertation (Massachusetts Institute of Technology/Woods Hole Oceanographic Institution, Woods Hole, Mass., 1995).
9. K. Y. H. Gin, S. W. Chisholm, and R. J. Olson, "Seasonal and depth variation in microbial size spectra at the Bermuda Atlantic time series station," Deep-Sea Res. I **46,** 1221–1245 (1999).
10. K. K. Cavender-Bares, "Size distributions, population dynamics, and single-cell properties of marine plankton in diverse nutrient environments," Ph.D. dissertation (Massachusetts Institute of Technology, Cambridge, Mass., 1999).
11. R. K. Y. Chan and K. M. Un, "Real-time size distribution, concentration, and biomass measurement of marine phytoplankton with a novel dual-beam laser fluorescence Doppler cytometer," Appl. Opt. **40,** 2956–2965 (2001).
12. S. G. Ackleson and R. W. Spinrad, "Size and refractive index of individual marine particulates: a flow cytometric approach," Appl. Opt. **27,** 1270–1277 (1988).
13. C. D. Mobley, *Light and Water; Radiative Transfer in Natural Waters* (Academic, San Diego, Calif., 1994).
14. M. J. Perry and S. M. Porter, "Determination of the cross-section absorption coefficient of individual phytoplankton cells by analytical flow cytometry," Limnol. Oceanogr. **34,** 1727–1738 (1989).
15. A. Bricaud, A. L. Bedhomme, and A. Morel, "Optical properties of diverse phytoplanktonic species: experimental results and theoretical interpretation," J. Plankton Res. **10,** 851–873 (1988).
16. M. D. DuRand and R. J. Olson, "Diel patterns in optical properties of the chlorophyte *Nannochloris* sp.: relating the indi-

vidual cell to bulk measurements," Limnol. Oceanogr. **43,** 1107–1118 (1998).
17. H. Volten, J. F. de Haan, J. W. Hovenier, R. Schreurs, W. Vassen, A. G. Dekker, H. J. Hoogenboom, F. Charlton, and R. Warts, "Laboratory measurements of angular distributions of light scattered by phytoplankton and silt," Limnol. Oceanogr. **43,** 1180–1197 (1998).
18. S. G. Ackleson, D. B. Robins, and J. A. Stephens, "Distributions in phytoplankton refractive index and size within the North Sea," in *Ocean Optics IX*, S. G. Ackleson, ed., Proc. SPIE **925,** 317–325 (1988).
19. W. S. Pegau, D. Gray, and J. R. V. Zaneveld, "Absorption and attenuation of visible and near-infrared light in water: dependence on temperature and salinity," Appl. Opt. **36,** 6035–6046 (1997).
20. R. A. Reynolds, D. Stramski, and D. A. Kiefer, "The effect of nitrogen limitation on the absorption and scattering properties of the marine diatom *Thalassiosira pseudonana*," Limnol. Oceanogr. **42,** 881–892 (1997).
21. D. Stramski and R. A. Reynolds, "Diel variations in the optical properties of a marine diatom," Limnol. Oceanogr. **38,** 1347–1364 (1993).
22. S. W. Jeffrey and N. A. Welschmeyer, "Spectrophotometric and fluorometric equations in common use in oceanography," in *Phytoplankton Pigments in Oceanography: Guidelines to Modern Methods*, S. W. Jeffrey, R. F. C. Mantoura, and S. W. Wright, eds. (UNESCO, Paris, 1997), pp. 597–615.
23. S. W. Wright, S. W. Jeffrey, and R. F. C. Mantoura, "Evaluation of methods and solvents for pigment extraction," in *Phytoplankton Pigments in Oceanography*, S. W. Jeffrey, R. F. C. Mantoura, and S. W. Wright, eds. (UNESCO, Paris, 1997), pp. 261–282.
24. A. Shalapyonok, R. J. Olson, and L. S. Shalapyonok, "Arabian Sea phytoplankton during Southwest and Northeast Monsoons 1995: composition, size structure and biomass from individual cell properties measured by flow cytometry," Deep-Sea Res. II **48,** 1231–1262 (2001).
25. M. D. DuRand, R. E. Green, H. M. Sosik, and R. J. Olson, "Diel variations in optical properties of *Micromonas pusilla* (Prasinophyceae)," J. Phycol. **38,** 1132–1142 (2002).
26. R. R. L. Guillard, "Culture of phytoplankton for feeding marine invertebrates," in *Culture of Marine Invertebrate Animals*, W. L. Smith and M. H. Chanely, eds. (Plenum, New York, 1975), pp. 29–60.
27. T. D. Dickey and A. J. Williams III, "Interdisciplinary ocean process studies on the New England shelf," J. Geophys. Res. **106,** 9427–9434 (2001).
28. H. M. Sosik, R. E. Green, W. S. Pegau, and C. S. Roesler, "Temporal and vertical variability in optical properties of New England shelf waters during late summer and spring," J. Geophys. Res. **106,** 9455–9472 (2001).
29. H. C. van de Hulst, *Light Scattering by Small Particles* (Wiley, New York, 1957).
30. A. Bricaud and A. Morel, "Light attenuation and scattering by phytoplankton cells: a theoretical modeling," Appl. Opt. **25,** 571–580 (1986).
31. C. F. Bohren and D. R. Hoffman, *Absorption and Scattering of Light by Small Particles* (Wiley, New York, 1983).
32. D. Stramski, "Refractive index of planktonic cells as a measure of cellular carbon and chlorophyll a content," Deep-Sea Res. I **46,** 335–351 (1999).
33. S. G. Ackleson and D. B. Robins, "Flow cytometric determinations of North Sea phytoplankton optical properties," Netherlands J. Sea Res. **25,** 11–18 (1990).
34. M. D. DuRand, R. J. Olson, and S. W. Chisholm, "Phytoplankton population dynamics at the Bermuda Atlantic Time-series station in the Sargasso Sea," Deep-Sea Res. II **48,** 1983–2003 (2001).
35. R. J. Olson, S. W. Chisholm, E. R. Zettler, M. A. Altabet, and J. A. Dusenberry, "Spatial and temporal distributions of prochlorophyte picoplankton in the North Atlantic Ocean," Deep-Sea Res. **37,** 1033–1051 (1990).
36. M. S. Twardowski, E. Bass, J. B. Macdonald, W. S. Pegau, A. H. Barnard, and J. R. Zaneveld, "A model for estimating bulk refractive index from the optical backscattering ratio and the implications for understanding particle composition in case I and case II waters," J. Geophys. Res. **106,** 14129–14142 (2001).
37. R. P. Bukata, J. H. Jerome, K. Y. Kondryatev, and D. V. Pozdnyakov, *Optical Properties and Remote Sensing of Inland and Coastal Waters* (CRC Press, Boca Raton, Fla., 1995).
38. B. G. Mitchell and D. A. Kiefer, "Chlorophyll *a* specific absorption and fluorescence excitation spectra for light-limited phytoplankton," Deep-Sea Res. **35,** 639–663 (1988).
39. H. M. Sosik, S. W. Chisholm, and R. J. Olson, "Chlorophyll fluorescence from single cells: interpretation of flow cytometric signals," Limnol. Oceanogr. **34,** 1749–1761 (1989).
40. H. M. Sosik and B. G. Mitchell, "Absorption, fluorescence and quantum yield for growth in nitrogen limited *Dunaliella tertiolecta*," Limnol. Oceanogr. **36** (5), 910–921 (1991).
41. K. Witkowski, T. Krol, and M. Lotocka, "The light scattering matrix of *Chlorella vulgaris* cells and its variability due to cell modification," Oceanologia **36,** 19–31 (1994).
42. K. Witkowski, T. Król, A. Zieliński, and E. Kuteń, "A light-scattering matrix for unicellular marine phytoplankton," Limnol. Oceanogr. **43,** 859–869 (1998).